EMBO reports

scientific report

Convergence of vitamin D and retinoic acid signalling at a common hormone response element

Luz Tavera-Mendoza[1], Tian-Tian Wang[2]*, Benjamin Lallemant[2], Rui Zhang[2], Yoshihiko Nagai[1,3], Véronique Bourdeau[2,4], Mario Ramiro Calderon[2], Julie Desbarats[2], Sylvie Mader[2,4] & John H. White[1,2+]*

[1]Department of Medicine, and [2]Department of Physiology, McGill University, Montreal, Quebec, Canada, [3]McGill University and Genome Quebec Innovation Centre, McGill University, Montreal, Quebec, Canada, and [4]Department of Biochemistry, University of Montreal, Montreal, Quebec, Canada

Although 1,25-dihydroxyvitamin D_3 ($1,25D_3$) and retinoic acid (RA) have distinct developmental and physiological roles, both regulate the cell cycle. We provide molecular and genomic evidence that their cognate nuclear receptors regulate common genes through everted repeat TGA(C/T)TPyN8PuG(G/T)TCA (ER8) response elements. ER8 motifs were found in the promoters of several target genes of $1,25D_3$ and/or RA. Notably, an element was characterized in the cyclin-dependent kinase (CDK) inhibitor *p19^{ink4d}* gene, and $1,25D_3$- or RA-induced $p19^{INK4D}$ expression. *P19^{ink4d}* knockdown together with depletion of *p27^{kip1}*, another CDK inhibitor regulated by $1,25D_3$ and RA, rendered cells resistant to ligand-induced growth arrest. Remarkably, $p19^{INK4D}$-deficient cells showed increased autophagic cell death, which was markedly enhanced by $1,25D_3$, but not RA, and attenuated by loss of $p27^{KIP1}$. These results show a limited crosstalk between $1,25D_3$ and RA signalling by means of overlapping nuclear receptor DNA binding specificities, and uncover a role for $p19^{INK4D}$ in control of cell survival.

Keywords: vitamin D; retinoic acid; nuclear receptors; autophagy; cross-talk; cyclin-dependent kinase inhibitors

EMBO reports (2006) **7**, 180–185. doi:10.1038/sj.embor.7400594

INTRODUCTION

Retinoic acid (RA) and the hormonal form of vitamin D3 (1,25-dihydroxyvitamin D_3; $1,25D_3$) signal through related nuclear receptors (Chawla *et al*, 2001). Both retinoic acid receptors (RARs) and the vitamin D receptor (VDR) heterodimerize with retinoid X receptors (RXRs). RAR/RXRs bind to retinoic acid response elements (RAREs) composed of direct repeats of PuG(G/T)TCA motifs separated by 1, 2 or 5 bp (DR1, DR2 or DR5), whereas vitamin D response elements (VDREs) are arranged as DR3 or weaker everted repeat (ER6) elements (Thompson *et al*, 2002). RAR signalling controls many aspects of embryonic development (Chambon 1996), whereas $1,25D_3$ is primarily known for its role in controlling mineral ion homeostasis. However, both $1,25D_3$ and RA regulate cell differentiation, proliferation and apoptosis (Freemantle *et al*, 2003; Lin & White, 2004), and show overlapping effects on the immune system (Stephensen, 2001; Lin & White, 2004).

A range of data has provided evidence for chemopreventive actions of $1,25D_3$ and its analogues, which show potent anticancer activities in *in vitro* and *in vivo* models (Lin & White, 2004). Similarly, vitamin A deficiency leads to squamous metaplasia of epithelia resembling early stages of carcinogenesis, and retinoids show chemotherapeutic and chemopreventive effects in cancers of the breast, liver and aerodigestive tract, and in acute promyelocytic leukaemia (Hong & Sporn, 1997; Freemantle *et al*, 2003).

We show here that ER8 elements function as VDREs and RAREs *in vitro* and *in vivo*, thus serving as a point of convergence of $1,25D_3$ and RA signalling. Scanning the human genome for promoter-proximal ER8 motifs showed elements in several previously identified $1,25D_3$ or RA target genes, including those encoding interleukin-10, the genotoxic stress-inducible factor DDIT3/GADD153/CHOP and the cyclin-dependent kinase (CDK) inhibitor $p19^{INK4D}$, which are responsive to both $1,25D_3$ and RA. Moreover, our results indicate that induction of $p19^{INK4D}$ contributes to the cell-cycle regulatory properties of $1,25D_3$ and RA, and, remarkably, protects cells against autophagic cell death.

RESULTS AND DISCUSSION

Identification of ER8 motifs as VDREs and RAREs

We identified $1,25D_3$ target genes in human SCC25 head and neck squamous cell carcinoma cells, the proliferation of which is arrested in G0/G1 by $1,25D_3$ and RA (Akutsu *et al*, 2001; Lin *et al*, 2002). In an analysis of $1,25D_3$ target genes, an everted repeat of

[1]Department of Medicine, and [2]Department of Physiology, McGill University, 3655 Drummond St, Montreal, Quebec, Canada H3G 1Y6
[3]McGill University and Genome Quebec Innovation Centre, McGill University, 740 Ave. Dr. Penfield, Montreal, Quebec, Canada H3G 1Y6
[4]Department of Biochemistry, University of Montreal, Montreal, Quebec, Canada H3C 3J7
*These authors should be considered as equal first authors
+Corresponding author. Tel: +1 514 398 8498; Fax: +1 514 398 7452;
E-mail: john.white@mcgill.ca

Received 11 May 2005; revised 25 October 2005; accepted 9 November 2005; published online 2 December 2005

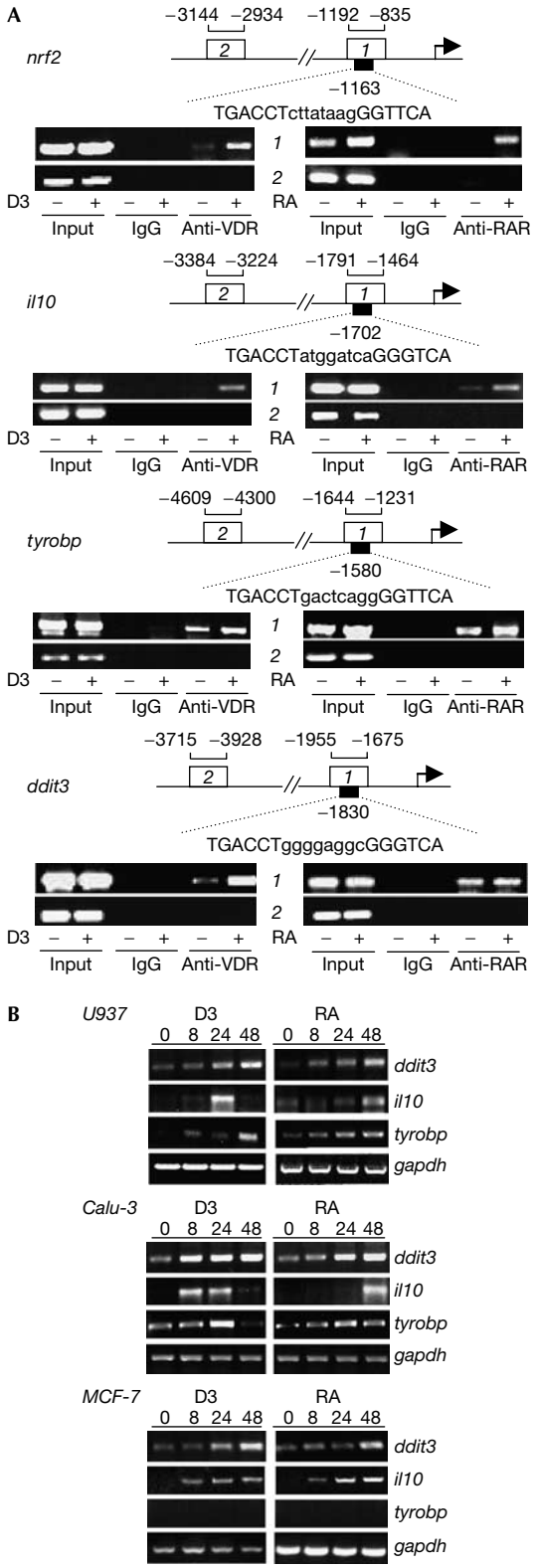

Fig 1 | Identification of ER8 elements in 1,25-dihydroxyvitamin D_3 and RA target genes. (**A**) Chromatin immunoprecipitation (ChIP) analysis of receptor binding to the ER8 element (region 1) of the *nrf2* promoter. Immunoprecipitation with nonspecific IgG and PCR amplification of an adjacent region (2) served as controls. ChIP assays were also carried out to analyse binding to ER8s in the *il10*, *ddit3* and *tyrobp* genes. RAR, retinoic acid receptor; VDR, vitamin D receptor. (**B**) Reverse transcription–PCR analysis of 1,25-dihydroxyvitamin D_3 ($1,25D_3$)- or retinoic acid (RA)-regulated expression of *ddit3*, *il10*, and *tyrobp* in U937, Calu-3 and MCF-7 cells.

PuG(G/T)TCA motifs separated by 8 bp (ER8) was identified in gene encoding transcription factor NRF2 (Fig 1A). Chromatin immunoprecipitation (ChIP) assays showed that the VDR bound to ER8 region of the *nfr2* promoter, but not to adjacent DNA (Fig 1A). Significantly, ER8 motifs also function as RAREs (Tini *et al*, 1993), and ligand-dependent binding of RARs to the ER8 region of the *nrf2* promoter was also detected by ChIP assay (Fig 1A).

We screened the human genome for ER8 motifs (Bourdeau *et al*, 2004; supplementary Table 1 online), and identified elements in several genes regulated by $1,25D_3$ and/or RA (supplementary Table 2 online). Apart from *nrf2* (*nfe2l2*; element at −1163), these include genes encoding thioredoxin reductase 1 (*txnrd1*; −1378), ETS variant 4 (*etv4/e1a-f*; −4233), TYROBP/DAP12 (*tyrobp*; −1580) and E4F1 (*e4f1*; +3102), identified as $1,25D_3$-regulated on microarrays (Lin *et al*, 2002), and *il10*, which is induced by $1,25D_3$ *in vivo* (Cobbold *et al*, 2003). The gene encoding CDK inhibitor $p19^{INK4D}$ (*cdkn2d*; −245) was identified as RA-regulated on microarrays (Liu *et al*, 2000). RA is also an inducer of RUNX1 (AML1; *runx1*; −1662; Tanaka *et al*, 1995) and human cholesteryl ester transfer protein (*cetp*; +418; Florentin *et al*, 1996), and both RA and $1,25D_3$ induce expression of keratin 13 (*krt13*; −3339; van Rossum *et al*, 2000; Palmer *et al*, 2003) and DDIT3 (CHOP, GADD153, C/EBPζ; *ddit3*; −1830; Kim *et al*, 2002; Lin *et al*, 2002).

Notably absent are *hox* genes, which are regulators of cell fate and embryonic patterning. RA, but not $1,25D_3$, regulates several *hox* genes, and DR2- or DR5-type RAREs are present in several *hox* promoters (Gellon & McGinnis, 1998). The absence of ER8 motifs in *hox* genes is consistent with the notion that flexibility in response element recognition would permit partially overlapping DNA binding specificities of different receptors, and thus limited crosstalk between receptor signalling pathways.

We further examined *il10* and *tyrobp*, which are not known to be regulated by RA, and *ddit3*, which is induced during growth arrest and in response to genotoxic and endoplasmic reticulum stress (Oyadomari & Mori, 2004). Interleukin-10, like $1,25D_3$, promotes immune system tolerance (Cobbold *et al*, 2003), and TYROBP is a transmembrane adaptor expressed throughout the immune system (Colonna, 2003). VDRs and RARs bind to ER8 regions of the *il10*, *tyrobp* and *ddit3* promoters in a ligand-dependent manner (Fig 1A). Regulation of gene expression was tested in ligand-responsive U937 myelomonocytic, Calu-3 lung carcinoma and MCF-7 breast cancer cells. With the exception of *tyrobp*, which was not detected in MCF-7 cells, expression of *il10*, *tyrobp* and *ddit3* was induced by $1,25D_3$ and RA in all cells (Fig 1B).

An ER8 element in the $p19^{INK4D}$ promoter

$P19^{INK4D}$ interacts selectively with CDK4, and its overexpression arrests cells in G0/G1 (Hirai *et al*, 1995). As we were interested in cell-cycle arrest by $1,25D_3$ and RA, we further analysed the regulation of $p19^{ink4d}$ and the function of its ER8 motif. Binding of VDR/RXRs to ER8 *in vitro* was analysed by electrophoretic

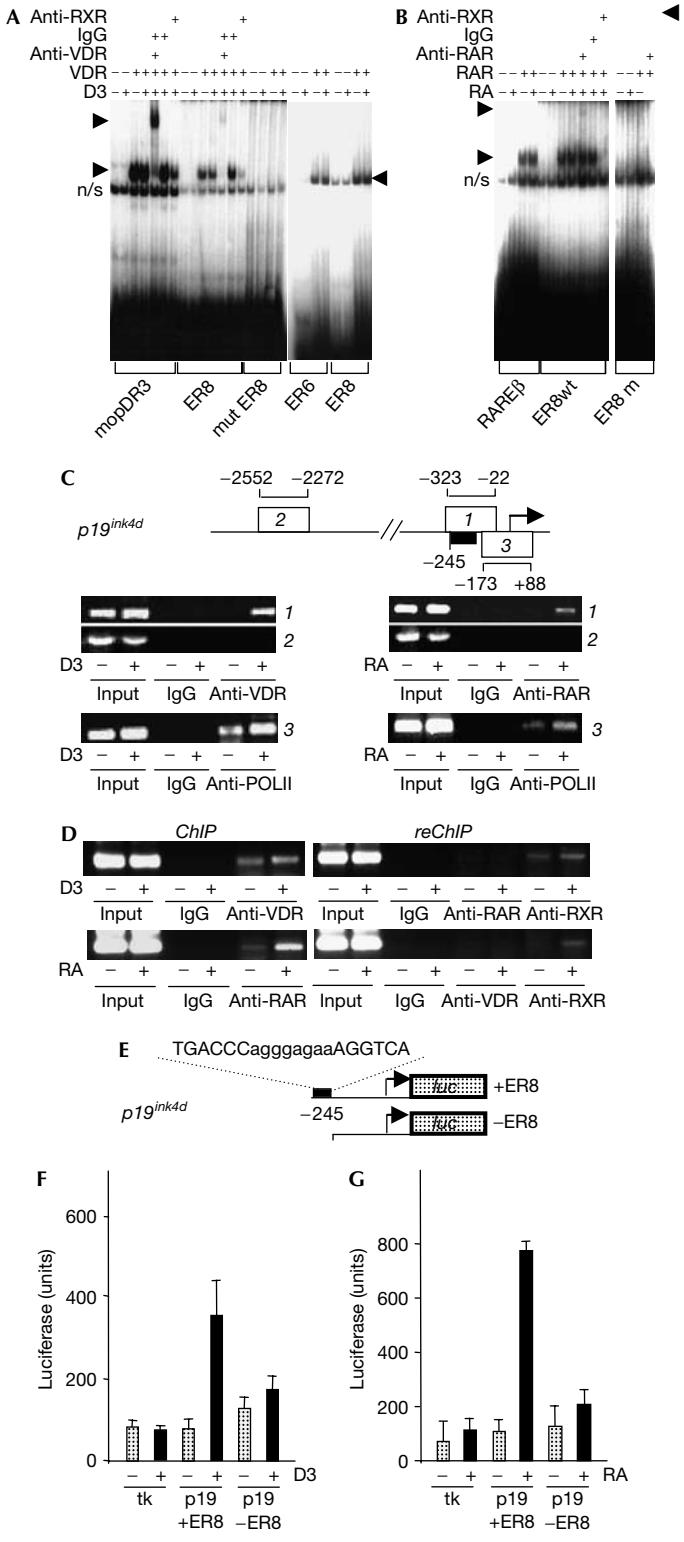

Fig 2 | Characterization of *in vitro* and *in vivo* $p19^{ink4d}$ ER8 element function. (**A**) Electrophoretic mobility shift assay (EMSA) of binding of vitamin D receptors (VDRs)/retinoid X receptors (RXRs) to the $p19^{ink4d}$ ER8, with binding to the mouse osteopontin (mop) DR3 vitamin D responsive element as a control, along with a comparison of binding to ER6 and ER8 motifs (right-hand panel). (**B**) EMSA of retinoic acid receptor (RAR)/RXR binding to the $p19^{ink4d}$ ER8, and the *rar*β DR5 retinoic acid response element, as a control. (**C**) Chromatin immunoprecipitation (ChIP) analysis of binding of VDRs and RARs to the $p19^{ink4d}$ ER8 (region 1) and RNA polymerase II (POLII) binding to the transcription start site. (**D**) ReChIP analysis confirms the presence of VDR/RXRs and RAR/RXRs but not of VDR/RARs on the $p19^{ink4d}$ ER8. (**E**) Cloning of $p19^{ink4d}$ promoter containing or lacking ER8 upstream of a *luciferase* reporter. 1,25-Dihydroxyvitamin D_3 ($1,25D_3$)- (**F**) and retinoic acid (RA)-regulated (**G**) luciferase expression is dependent on the ER8 element in the $p19^{ink4d}$ promoter. Luciferase expression driven by a thymidine kinase (tk) control promoter is shown.

mobility shift assay (EMSA) using the mouse osteopontin (*mop*) DR3 or the weaker *cyp3A4* ER6 VDRE as controls (Fig 2A). VDR-specific complex formation on the ER8 motif was super-shifted or partially disrupted by antibodies against VDRs and RXRs, respectively. VDR binding to the ER8 element was weaker than to the DR3 VDRE, but comparable with binding to the ER6 VDRE. Similar analysis of RAR binding using the *rar*β DR5 RARE as a control (Fig 2B) confirmed that RAR/RXRs bound strongly to the ER8 motif. Ligand-dependent binding of VDRs and RARs to the $p19^{ink4d}$ promoter was confirmed *in vivo*, and treatment with either ligand enhanced the interaction of RNA polymerase II with the initiation site of the $p19^{ink4d}$ promoter (Fig 2C). ReChIP experiments showed that receptors bound as heterodimers with RXRs, whereas no evidence was found for binding of VDR/RAR heterodimers to ER8 (Fig 2D). Moreover, the integrity of the ER8 motif was essential for $1,25D_3$- or RA-dependent induction of a $p19^{ink4d}$ promoter-*luciferase* reporter (Fig 2E–G), confirming the function of the element. Finally, transfection of RARs α, β or γ produced similar fold inductions of reporter activity (supplementary Fig 1 online), and no evidence for synergism between RA and $1,25D_3$ was found (data not shown).

Rapid induction of $p19^{ink4d}$ messenger RNA was observed in four $1,25D_3$- and RA-sensitive cell lines (Fig 3A), and treatment with either ligand increased $p19^{INK4D}$ protein levels in U937, SCC25 or Calu-3 cells in 48 h (Fig 3B; data not shown). This coincided with a transient increase in the association of $p19^{INK4D}$ with CDK4 in U937 and SCC25 cells, although levels of CDK4 were not affected (Fig 3C; data not shown). In contrast, a more gradual and sustained increase in $p27^{KIP1}$/CDK4 complexes was observed in $1,25D_3$-treated cells (Fig 3D), which suggested that the two CDK inhibitors function cooperatively.

SiRNA knockdown of $p19^{INK4D}$ and $p27^{KIP1}$

We were interested in determining whether induction of $p19^{INK4D}$ contributed to cell-cycle regulation by $1,25D_3$ and RA, and whether it cooperated with $p27^{KIP1}$, another $1,25D_3$- and RA-induced CDK inhibitor. $P19^{INK4D}$ expression was knocked down by short interfering RNAs (siRNAs) to test its role in $1,25D_3$- and RA-regulated SCC25 cell proliferation (Akutsu *et al*, 2001). SCC25 cells were transfected with siRNAs with almost 100% efficiency (supplementary Fig 2 online), and complete $p19^{INK4D}$ knockdown was achieved, whereas no effect of either scrambled RNA or cyclophilin-specific siRNA was observed (Fig 4A; data not shown). Complete knockdown of $p27^{KIP1}$ also occurred, alone and in combination with $p19^{INK4D}$ (Fig 4B). $1,25D_3$ treatment of cells transfected with scrambled siRNA reduced cells in S phase and

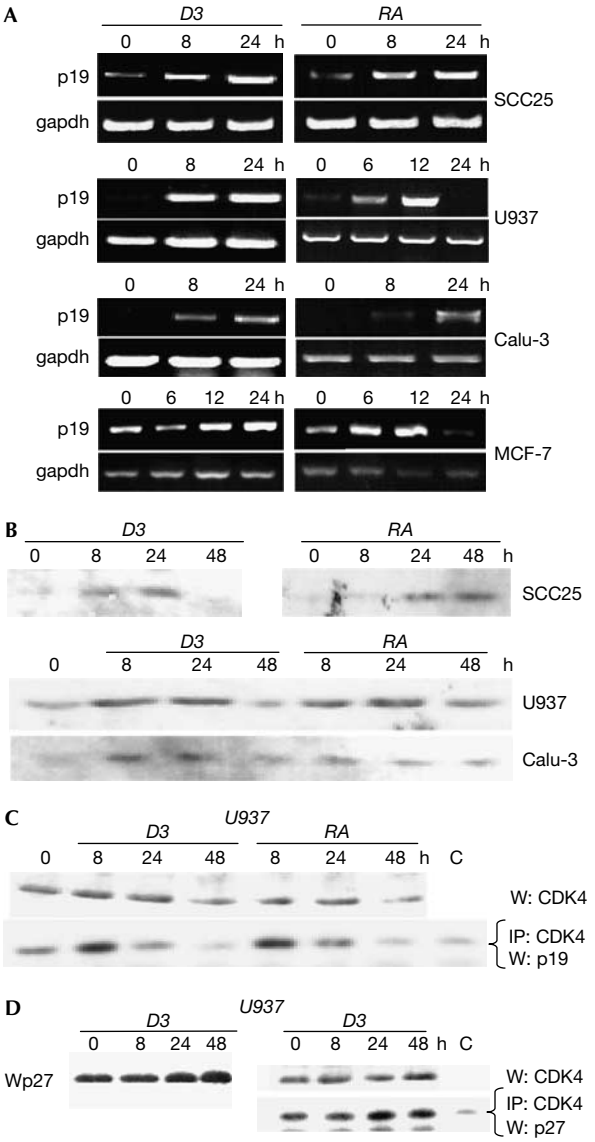

Fig 3 | 1,25-dihydroxyvitamin D_3 and retinoic acid induce *p19^{ink4d}* expression. Expression of *p19^{ink4d}* messenger RNA by reverse transcription–PCR (**A**) or protein by western blotting (**B**) was carried out on extracts of cells treated with 1,25-dihydroxyvitamin D_3 ($1,25D_3$) or retinoic acid (RA), as indicated. (**C**) Treatment with $1,25D_3$ or RA transiently enhances co-immunoprecipitation (IP) of $p19^{INK4D}$ with cyclin-dependent kinase (CDK)4 in U937 cells. Similar results were obtained in SCC25 cells (not shown). A control western blot (W) of CDK4 levels in ligand-treated cells is shown below. (**D**) Treatment with $1,25D_3$ enhances co-immunoprecipitation of $p27^{KIP1}$ with CDK4 in U937 cells. Extracts of U937 cells were probed for $p27^{KIP1}$ and CDK4, and immunoprecipitated with an anti-CDK antibody and probed for $p27^{KIP1}$ co-immunoprecipitation.

increased cells in sub-G0/G1 (Fig 4C), suggestive of cytotoxicity. Remarkably, $p19^{INK4D}$ knockdown substantially reduced cell survival (supplementary Fig 3A online) and increased the sub-G0/G1 fraction (Fig 4C), an effect that was markedly enhanced by $1,25D_3$, indicating that $p19^{INK4D}$ expression protects cells from ($1,25D_3$-induced) cell death. Surviving $p19^{INK4D}$-depleted cells treated with $1,25D_3$ showed enhanced Trypan blue uptake, consistent with decreased viability (supplementary Fig 3B online). In contrast, $p27^{KIP1}$ knockdown reduced the G0/G1 fraction, slightly enhanced cells in S and substantially increased cells in G2/M (Fig 4C), effects that were modestly reversed by $1,25D_3$. Combined loss of $p19^{INK4D}$ and $p27^{KIP1}$ produced a cell-cycle distribution that was similar to that of $p27^{KIP1}$-depleted cells (Fig 4C), indicating that $p27^{KIP1}$ loss reverses the sensitivity to cell death caused by $p19^{INK4D}$ depletion. Although $1,25D_3$ treatment somewhat reduced cells in G2/M, the proportion of $p19^{INK4D}$/$p27^{KIP1}$-depleted cells in S phase remained elevated, consistent with a role for the two CDK inhibitors in $1,25D_3$-induced G0/G1 arrest. In contrast, RA treatment of $p19^{INK4D}$-depleted cells substantially reduced the sub-G0/G1 fraction (Fig 4D). However, there was double the proportion of cells in S phase relative to controls, consistent with *p19^{ink4d}* induction contributing to RA-induced cell-cycle arrest. Similarly, the proportion of cells in S phase remained elevated in RA-treated cells depleted for $p27^{KIP1}$, or both $p19^{INK4D}$ and $p27^{KIP1}$ (Fig 4D).

Cell death observed in $p19^{INK4D}$-depleted cells was not accompanied by enhanced caspase-3 cleavage or annexin V staining (supplementary Fig 4 online; data not shown), indicating that cell death was not apoptotic. No β-galactosidase activity characteristic of senescence (pH 6.0; Dimri *et al*, 1995) was detected (data not shown). However, as cell shrinkage and cytoplasmic vacuolization were observed, we investigated whether cells were dying by autophagy. The combination of $p19^{INK4D}$ loss and $1,25D_3$ treatment markedly enhanced the proportion of cells expressing high levels of lysosomal β-galactosidase activity (pH 4.0; Fig 4E). Moreover, although $1,25D_3$ treatment or siRNA transfection tended to increase lysosomal numbers in SCC25 cells, as judged by lysotracker red incorporation, vacuolization was only observed in $p19^{INK4D}$-depleted cells (Fig 4F). The effect, however, is cell specific, as $p19^{INK4D}$ knockdown in U937 cells neither significantly affected cell viability (data not shown) nor ligand-induced U937 differentiation (supplementary Fig 5 online), an unexpected result given the induction of macrophage differentiation by $p19^{INK4D}$ overexpression in immature myeloid cells (Adachi *et al*, 1997).

Conclusions

We found that $1,25D_3$ and RA regulate common target genes, including *p19^{ink4d}*, by recognizing ER8 motifs as response elements. Induction of *p19^{ink4d}* contributes to cell-cycle regulation by $1,25D_3$ and RA, and emphasizes the overlapping effects of $1,25D_3$ and RA on cell-cycle regulators. Both enhance expression of $p19^{INK4D}$ and $p27^{KIP1}$, although by distinct mechanisms. $1,25D_3$ or RA treatment increases $p27^{KIP1}$ protein expression by repressing levels of transcripts encoding $p45^{SKP2}$, a ubiquitin ligase that targets KIP1 for proteasomal degradation (Dow *et al*, 2001; Lin *et al*, 2003). We found that cells lacking both $p19^{INK4D}$ and $p27^{KIP1}$ are refractory to $1,25D_3$ and RA, and that the two CDK inhibitors cooperate in ligand-mediated cell-cycle regulation. Cooperation between $p19^{INK4D}$ and $p27^{KIP1}$ is supported by genetic studies, where they were combined to control mouse postnatal neuronal (Zindy *et al*, 1999) and retinal cell proliferation (Cunningham *et al*, 2002).

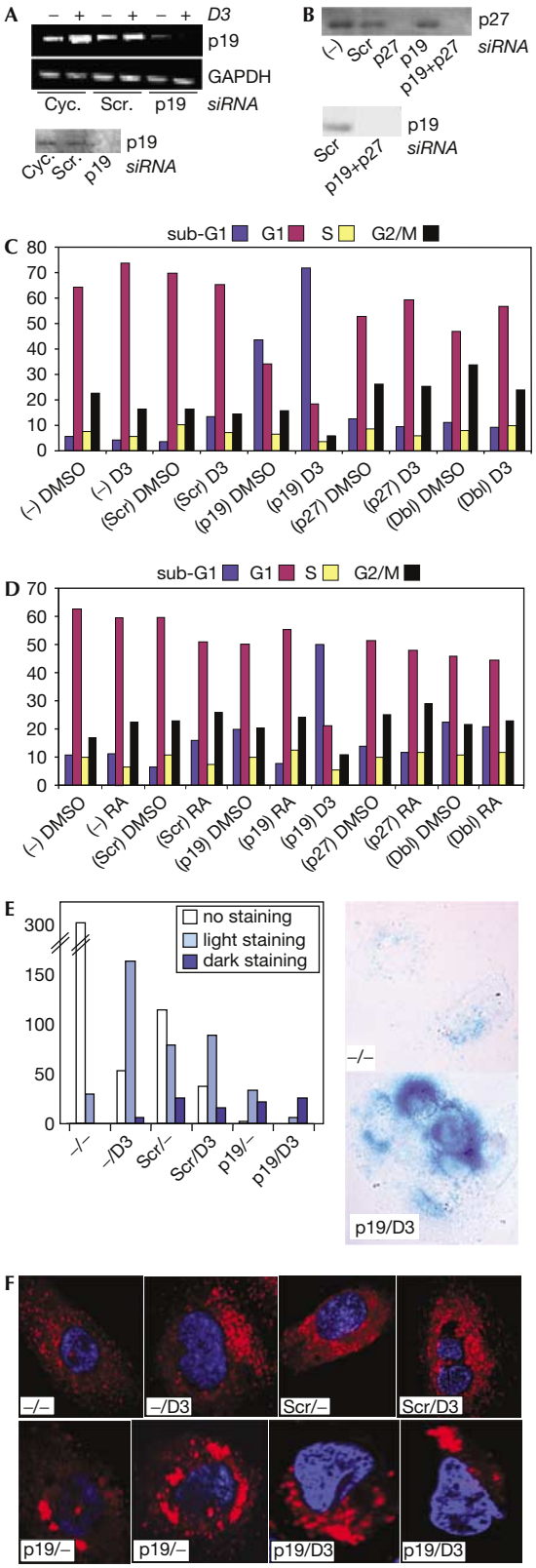

Fig 4 | Knockdown of *p19*^{ink4d} and *p27*^{kip1} in SCC25 cells. (**A**) Short interfering RNAs (siRNA) knockdown of *p19*^{ink4d} messenger RNA and protein in SCC25 cells. SiRNAs were directed against *p19*^{ink4d}, scrambled *p19*^{ink4d} (Scr.) or cyclophilin (cyc.) controls. (**B**) Combined knockdown of $p27^{KIP1}$ and $p19^{INK4D}$ in SCC25 cells analysed by western blotting for $p27^{KIP1}$ (top) and $p19^{INK4D}$ (bottom). (**C**,**D**) Fluorescence-activated cell sorting analysis of cell-cycle distribution of control SCC25 cells, or cells transfected with scrambled (Scr), *p19*^{ink4d}- or *p27*^{kip1}-directed siRNAs, individually or together (Dbl). (**C**) Cells were treated with vehicle or 1,25-dihydroxyvitamin D_3 ($1,25D_3$), as indicated. (**D**) Cells were treated with DMSO vehicle, retinoic acid (RA) or $1,25D_3$, as indicated. (**E**) Loss of $p19^{INK4D}$ enhances lysosomal β-galactosidase activity in SCC25 cells. (Left) Histogram of numbers of cells staining for β-galactosidase activity in the absence (−) or presence of $1,25D_3$ in control cells (−) or in cells transfected with scrambled (Scr) or $p19^{INK4D}$ siRNAs. (Right) Bright field images of untransfected cells (−/−) or $p19^{INK4D}$-depleted cells treated with $1,25D_3$ (p19/D3). (**F**) Loss of $p19^{INK4D}$ induces lysosomal fusion. Analysis of lysosomal fusion (autophagosomes) in SCC25 cells treated as in (**E**), stained for incorporation of lysotracker red. Nuclei were counterstained with Hoechst (blue).

Remarkably, loss of *p19*^{ink4d} rendered cells more sensitive to autophagic cell death, an effect that was markedly enhanced by $1,25D_3$, but not by RA. These results are consistent with autophagic cell death observed in $1,25D_3$-treated MCF-7 cells (Hoyer-Hansen *et al*, 2005), and show a role for $p19^{INK4D}$ induction in protecting cells from death induced by autophagy. These results are also noteworthy in the light of observations that induction of $p19^{INK4D}$ confers resistance to UV-induced apoptosis, and, importantly, enhances DNA repair (Ceruti *et al*, 2005). Induction of $p19^{INK4D}$ may thus be one of the components of the protective effects of $1,25D_3$ and RA against UV damage in epithelia, and would, in part, explain their chemopreventive properties. We also found that $p19^{INK4D}$-depleted SCC25 cells were hypersensitive to UV-induced apoptosis, as measured by annexin V and propidium iodide co-staining (unpublished results).

The autophagic phenotype of $p19^{INK4D}$ depletion is striking, given the contrast with the hyperproliferative response in cells lacking other INK4 proteins (Bond *et al*, 2004). Gene knockouts have not supported a role for *p19*^{ink4d} in tumour suppression. However, combined loss of $p19^{INK4D}$ and $p27^{KIP1}$ in our study did not result in autophagy, but led to resistance to ligand-induced cell-cycle arrest. Combined loss of $p19^{INK4D}$ and $p27^{KIP1}$ in mice led to postnatal death associated with neuronal defects (Zindy *et al*, 1999), thus preventing analyses of long-term effects of combined depletion on cancer susceptibility. It therefore remains possible that loss of both CDKs could promote aberrant cell proliferation during tumorigenesis.

METHODS

Details of cell culture, plasmids, transfections, ChIP assays, cell-cycle analysis, primers and antibodies used are found in the supplementary information online.

Response element screening. Screening was carried out as described by Bourdeau *et al* (2004) using NCBI fasta and gbs files of the Human genome reference assembly (Build 35 version 1; 26 August 2004) to search for specified sequences and extract the positions of matching motifs in the genome contigs, as well as the coordinates of the surrounding genes within a preset cutoff distance of each motif.

Short interfering RNA knockdowns. SCC25 cells, grown in 6 cm wells to a density of 2×10^5 cells/well, were transfected in

OPTI-MEM (Invitrogen, Burlington, Ontario, Canada) with Oligofectamine (Invitrogen) and 100 nM of scrambled, *p19^{ink4d}* or *p27^{kip1}* siRNAs (Dharmacon, Lafayette, CO, USA). DMEM/F12 with 30% fetal bovine serum was added 6 h after transfection. After 24 h, the medium was replaced by DMEM/F12 with 10% fetal bovine serum for 24 h, followed by a medium containing charcoal-stripped serum (10%) and DMSO, 1,25D_3 (100 nM) or RA (1 μM) for 48 h. Cells were collected for fluorescence-activated cell sorting (FACS) analysis.

Microscopy. Cells were stained for lysosomal β-galactosidase (Dimri *et al*, 1995), and bright field digital images were captured using a Zeiss Axioplan 2 microscope, equipped with motorized stage and focus, and Zeiss AxioCamHRC digital camera coupled to AxioVision 4 software (Zeiss, Canada). Confocal microscopy was carried out using a Zeiss LSM 510 microscope with a two-photon titanium:sapphire laser. Samples were stained with lysotracker red DND99 and counterstained with Hoechst dye (Molecular Probes, Eugene, OR, USA).

Supplementary information is available at *EMBO reports* online (http://www.emboreports.org).

ACKNOWLEDGEMENTS

We are grateful to Dr D. Maysinger, J. Laliberté and K. Bell for help with cytochemistry and confocal microscopy, and to K. MacDonald for help with FACS. This work was supported by grants from the Canadian Institutes of Health Research (CIHR) to J.H.W. and from the Natural Sciences and Engineering Research Council to S.M. J.H.W. and S.M. are Chercheurs-Boursier of the Fonds de Recherché en Santé du Québec. L.T.M. was supported by a training grant from the CIHR. V.B. was supported by Genome Canada and the CIHR. S.M. is the holder of a Canadian Imperial Bank of Commerce Breast Cancer Research Chair.

REFERENCES

Adachi M, Roussel MF, Havenith K, Sherr CJ (1997) Features of macrophage differentiation induced by p19^{INK4D}, a specific inhibitor of cyclin D-dependent kinases. *Blood* **90:** 126–137

Akutsu N, Lin R, Bastien Y, Bestawros A, Enepekides DJ, Black MJ, White JH (2001) Regulation of gene expression by 1α,25-dihydroxyvitamin D_3 and its analog EB1089 under growth inhibitory conditions in squamous carcinoma cells. *Mol Endocrinol* **15:** 1127–1139

Bond J, Jones C, Haughton M, DeMicco C, Kipling D, Wynford-Thomas D (2004) Direct evidence from siRNA-directed 'knock down' that p16(INK4a) is required for human fibroblast senescence and for limiting ras-induced epithelial cell proliferation. *Exp Cell Res* **292:** 151–156

Bourdeau V, Deschenes J, Metivier R, Nagai Y, Nguyen D, Bretschneider N, Gannon F, White JH, Mader S (2004) Genome-wide identification of high affinity estrogen response elements in human and mouse. *Mol Endocrinol* **18:** 1411–1427

Ceruti JM, Scassa ME, Flo JM, Varone CL, Canepa ET (2005) Induction of p19INK4d in response to ultraviolet light improves DNA repair and confers resistance to apoptosis in neuroblastoma cells. *Oncogene* **24:** 4065–4080

Chambon P (1996) A decade of molecular biology of retinoic acid receptors. *FASEB J* **10:** 940–954

Chawla A, Repa J, Evans RM, Mangelsdorf DJ (2001) Nuclear receptors and lipid physiology: opening the X-files. *Science* **294:** 1866–1870

Cobbold SP *et al* (2003) Regulatory T cells and dendritic cells in transplantation tolerance: molecular markers and mechanisms. *Immunol Rev* **196:** 109–124

Colonna M (2003) Trems in the immune system and beyond. *Nat Rev Immunol* **3:** 445–453

Cunningham JJ, Levine EM, Zindy F, Goloubeva O, Roussel MF, Smeyne RJ (2002) The cyclin-dependent kinase inhibitors p19(Ink4d) and p27(Kip1) are coexpressed in select retinal cells and act cooperatively to control cell cycle exit. *Mol Cell Neurosci* **19:** 359–374

Dimri GP *et al* (1995) A biomarker that identifies senescent human cells in culture and in aging skin *in vivo*. *Proc Natl Acad Sci USA* **92:** 9363–9367

Dow R, Hendley J, Pirkmaier A, Musgrove EA, Germain D (2001) Retinoic acid-mediated growth arrest requires ubiquitylation and degradation of the F-box protein Skp2. *J Biol Chem* **276:** 45945–45951

Florentin E, Athias A, Lagrost L (1996) Modulation of the activity of the human cholesteryl ester transfer protein by carboxylated derivatives—evidence for 13-*cis*-retinoic acid as a potent activator of the protein's activity in plasma. *Eur J Biochem* **240:** 699–706

Freemantle SJ, Spinella MJ, Dmitrovsky E (2003) Retinoids in cancer therapy and chemoprevention: promise meets resistance. *Oncogene* **22:** 7305–7315

Gellon G, McGinnis W (1998) Shaping animal body plans in development and evolution by modulation of Hox expression patterns. *Bioessays* **20:** 116–125

Hirai H, Roussel M, Kato JY, Ashmun RA, Sherr CJ (1995) Novel INK4 proteins p18 and p19 are specific inhibitors of the cyclin D-dependent kinases CDK4 and CDK6. *Mol Cell Biol* **15:** 2762–2781

Hong WK, Sporn MB (1997) Recent advances in chemoprevention of cancer. *Science* **278:** 1073–1077

Hoyer-Hansen M, Bastholm L, Mathiasen IS, Elling F, Jaattela M (2005) Vitamin D analog EB1089 triggers dramatic lysosomal changes and beclin 1-mediated autophagic cell death. *Cell Death Differ* **12:** 1297–1309

Kim DG, You KR, Liu MJ, Choi YK, Won YS (2002) GADD153-mediated anticancer effects of *N*-(4-hydroxyphenyl)retinamide on human hepatoma cells. *J Biol Chem* **277:** 38930–38938

Lin R, White JH (2004) The pleiotropic actions of vitamin D. *Bioessays* **26:** 21–28

Lin R, Nagai Y, Sladek R, Bastien Y, Ho J, Petrecca K, Sotiropoulou G, Diamandis EP, Hudson TJ, White JH (2002) Expression profiling in squamous carcinoma cells reveals pleiotropic effects of vitamin D3 signaling on cell proliferation, differentiation and immune system regulation. *Mol Endocrinol* **16:** 1243–1256

Lin R, Wang TT, Miller WH, White JH (2003) Inhibition of F-box protein p45^{SKP2} expression and stabilization of cyclin-dependent kinase inhibitor p27^{KIP1} in vitamin D analogue-treated cancer cells. *Endocrinology* **144:** 749–753

Liu TX *et al* (2000) Gene expression networks underlying retinoic acid-induced differentiation of acute promyelocytic leukemia cells. *Blood* **96:** 1496–1504

Oyadomari S, Mori M (2004) Roles of CHOP/GADD153 in endoplasmic reticulum stress. *Cell Death Differ* **11:** 381–389

Palmer HG, Sanchez-Carbayo M, Ordonez-Moran P, Larriba MJ, Cordn-Cardo C, Munoz A (2003) Genetic signatures of differentiation induced by 1α,25-dihydroxyvitamin D-3 in human colon cancer cells. *Cancer Res* **63:** 7799–7806

Stephensen CB (2001) Vitamin A, infection, and immune function. *Annu Rev Nutr* **21:** 167–192

Tanaka K, Tanaka T, Ogawa S, Kurokawa M, Mitani K, Yazaki Y, Hirai H (1995) Increased expression of aml1 during retinoic-acid-induced differentiation of U937 cells. *Biochem Biophys Res Commun* **211:** 1023–1030

Thompson PD, Jurutka PW, Whitfield GK, Myskowski SM, Eichhorst KR, Dominguez CE, Haussler CA, Haussler MR (2002) Liganded VDR induces CYP3A4 in small intestinal and colon cancer cells via DR3 and ER6 vitamin D responsive elements. *Biochem Biophys Res Commun* **299:** 730–738

Tini M, Otulakowski G, Breitmen ML, Tsui LC, Giguère V (1993) An everted repeat mediates retinoic acid induction of the γ-F-crystallin gene—evidence of a direct role for retinoids in lens development. *Genes Dev* **7:** 295–307

van Rossum MM, Mommers JM, van de Kerkhof PCM, van Erp PEJ (2000) Coexpression of keratins 13 and 16 in human keratinocytes indicates association between hyperproliferation-associated and retinoid-induced differentiation. *Arch Dermatol Res* **292:** 16–20

Zindy F, Cunningham JJ, Sherr CJ, Jogal S, Smeyne RJ, Roussel MF (1999) Postnatal neuronal proliferation in mice lacking Ink4d and Kip1 inhibitors of cyclin-dependent kinases. *Proc Natl Acad Sci USA* **96:** 13462–13467